

An All-Recombinant Protein-Based Culture System Specifically Identifies Hematopoietic Stem Cell Maintenance Factors

Aki Ieyasu,¹ Reiko Ishida,¹ Takaharu Kimura,¹ Maiko Morita,¹ Adam C. Wilkinson,^{1,4} Kazuhiro Sudo,² Toshinobu Nishimura,⁴ Jun Ohehara,¹ Yoko Tajima,¹ Chen-Yi Lai,¹ Makoto Otsu,¹ Yukio Nakamura,² Hideo Ema,³ Hiromitsu Nakauchi,^{1,4,*} and Satoshi Yamazaki^{1,5,*}

¹Laboratory of Stem Cell Therapy, Center for Experimental Medicine, The Institute of Medical Science, The University of Tokyo, Tokyo 108-8639, Japan

²Cell Engineering Division, BioResource Center, RIKEN, 3-1-1 Koyadai, Tsukuba, Ibaraki 305-0074, Japan

³Institute of Hematology and Blood Diseases Hospital, Chinese Academy of Medical Sciences and Peking Union Medical College, 288 Nanjing Road, Tianjin 300020, China

⁴Institute for Stem Cell Biology and Regenerative Medicine, Stanford University School of Medicine, Lorry I. Lokey Stem Cell Research Building, 265 Campus Drive, Stanford, CA 94305-5461, USA

⁵Project Division of Advanced Regenerative Medicine, The Institute of Medical Science, the University of Tokyo, Tokyo 108-8639, Japan

*Correspondence: nakauchi@ims.u-tokyo.ac.jp (H.N.), y-sato4@ims.u-tokyo.ac.jp (S.Y.)

<http://dx.doi.org/10.1016/j.stemcr.2017.01.015>

SUMMARY

Hematopoietic stem cells (HSCs) are considered one of the most promising therapeutic targets for the treatment of various blood disorders. However, due to difficulties in establishing stable maintenance and expansion of HSCs *in vitro*, their insufficient supply is a major constraint to transplantation studies. To solve these problems we have developed a fully defined, all-recombinant protein-based culture system. Through this system, we have identified hemopexin (HPX) and interleukin-1 α as responsible for HSC maintenance *in vitro*. Subsequent molecular analysis revealed that HPX reduces intracellular reactive oxygen species levels within cultured HSCs. Furthermore, bone marrow immunostaining and 3D immunohistochemistry revealed that HPX is expressed in non-myelinating Schwann cells, known HSC niche constituents. These results highlight the utility of this fully defined all-recombinant protein-based culture system for reproducible *in vitro* HSC culture and its potential to contribute to the identification of factors responsible for *in vitro* maintenance, expansion, and differentiation of stem cell populations.

INTRODUCTION

Hematopoietic stem cells (HSCs) maintain the ability to self-renew and differentiate within their *in vivo* microenvironment, the bone marrow (BM). From a clinical perspective, HSCs are important because they can generate the full blood cell repertoire upon transplantation (Eaves, 2015) and are therefore critical determinants of clinical BM transplant success. Additionally, in combination with gene therapy approaches HSCs also offer the significant potential to treat a range of inherited hematological disorders. However, our ability to maintain and expand HSCs outside of their *in vivo* microenvironment is currently limited.

The current protocols for *ex vivo* expansion of HSCs can be broadly divided into two groups, based on their use of cell-intrinsic or cell-extrinsic factors (Walasek et al., 2012). Cell-intrinsic factors include exogenous expression transcription factors such as HoxB4 (Sauvageau et al., 1995), and chromatin remodeling factors such as Bmi1 (Iwama et al., 2004). Such approaches have to date required genetic modification that limits their direct translational application. By contrast, cell-extrinsic factors such as cytokines are simply added to the culture media and act on unmodified HSCs.

Cytokines and other extrinsic factors are present in the specialized BM microenvironments, the so-called

BM niche, and are thought to be involved in migration, quiescence, and differentiation of HSCs (Kiel and Morrison, 2008). Many different cell types have been proposed as the candidate for the BM niche, including osteoblasts (Calvi et al., 2003; Zhang et al., 2003), endothelial cells (Kiel et al., 2005), chemokine ligand 12 (CXCL12)-abundant reticular cells (Sugiyama et al., 2006), mesenchymal stem cells (Mendez-Ferrer et al., 2010), and non-myelinating Schwann glial cells (Yamazaki et al., 2006, 2011).

BM niche cells are thought to secrete numerous factors such as stem cell factor (SCF) (Barker, 1994) and thrombopoietin (TPO) (Ku et al., 1996), which are generally necessary for HSC maintenance. These cytokines have long been added to culture media to investigate HSC proliferation and reconstitution ability. However, there are concerns about data reproducibility between laboratories, with such discrepancies often being ascribed to differences in experimental culture conditions.

HSCs have been widely analyzed using liquid or methylcellulose culture in the presence of fetal bovine serum (FBS). FBS contains myriad of growth factors, adhesion molecules, and other components, and also protects cells from rapid changes in pH. However, because of the high degree of unknown factors, FBS is now often replaced with serum-free medium containing BSA fraction V (BSA-FV;

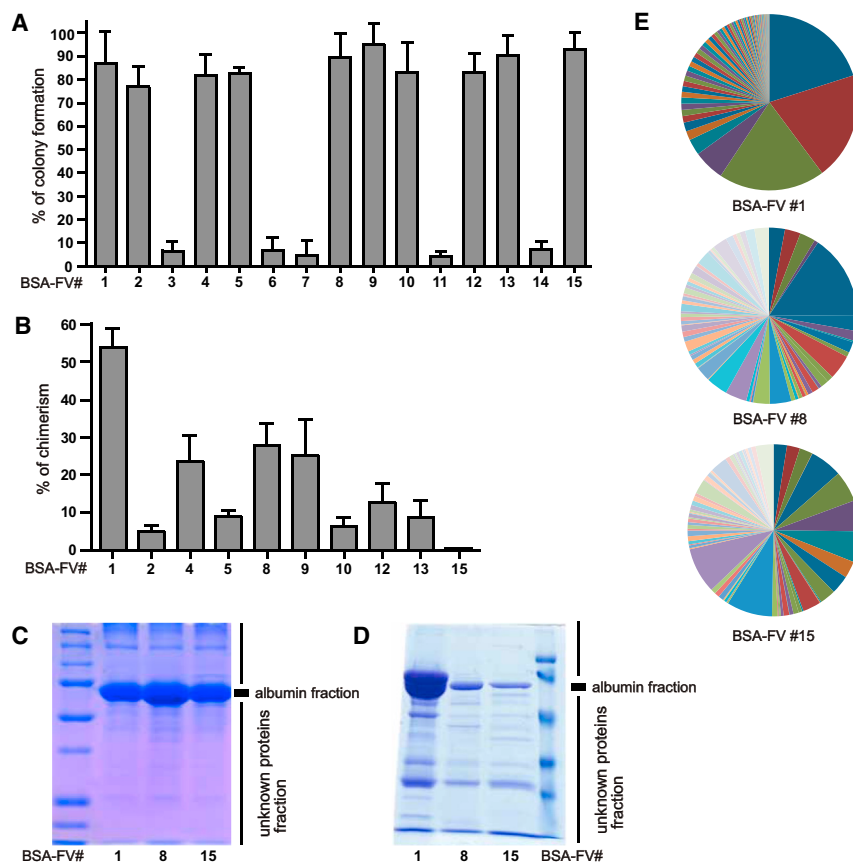


Figure 1. Heterogeneity in BSA-FV Lots Affects HSC Maintenance

(A) Percentage of single CD34⁺ HSCs forming colonies after in vitro culture for 11 days with cytokines and various BSA-FV lots. Mean \pm SEM from three independent experiments (n = 30 per BSA-FV culture condition). (B) Percentage peripheral blood (PB) chimerism from 40 CD34⁺ KSL cells, cultured for 1 week with cytokines and various BSA-FV lots and transplanted into lethally irradiated recipients together with 10⁶ bone marrow (BM) competitor cells. PB chimerism 12 weeks after transplantation. Mean \pm SD of three independent experiments (n = 10 mice per BSA-FV culture condition). (C and D) Protein analysis of total BSA-FV (C) and albumin-depleted BSA-FV (D) by SDS-PAGE. (E) The ratio of proteins identified by HPLC-MS analyses in different lots of BSA-FV (BSA-FV #1, #8, #15), excluding albumin.

the fifth ethanol fraction in the original purification process of plasma proteins) (Guilbert and Iscove, 1976) for in vitro HSC culture. BSA-based serum-free cultures have been well established for pluripotent stem cells. However, stable in vitro expansion of HSCs remains difficult and non-reproducible. This is at least in part due to the use of different batches (lots) of BSA-FV by different laboratories.

To address these issues, we tested 15 different lots of commercially available BSA-FV; each exhibited different abilities to maintain HSCs and unique protein profiles. To identify the best molecular candidates for HSC maintenance in BSA-FV, we developed a fully defined culture system using all-recombinant proteins. Using this approach, we provide evidence that HSC maintenance is strongly supported by two factors in BSA-FV, interleukin-1 α (IL-1 α) and hemopexin (HPX). Further investigation found that HPX reduced HSC intracellular reactive oxygen species (ROS) levels and that HPX was present on non-myelinating Schwann cells, a constituent of HSC niche in BM. These findings highlight the utility of all-recombinant protein-based systematic analysis for ex vivo HSC self-renewal and differentiation, and identification of bona fide growth factors that contribute to these cell-fate decisions.

RESULTS

HSC Maintenance Depends on Varying Levels of Unidentified Proteins Contained in BSA-FV

During our attempts at in vitro maintenance of HSCs, we realized that different BSA-FV lots varied tremendously in their colony-forming ability. We therefore evaluated 15 different lots of BSA-FV based on the ability to support colony formation from single CD34⁺ KSL HSCs (Osawa et al., 1996). After 11 days in culture with each BSA-FV lot, we confirmed that 5 out of 15 lots showed very poor colony-formation ability (Figure 1A). We next cultured HSCs with the remaining ten lots of BSA-FV for 1 week and examined their blood system repopulating potential using competitive repopulation assays. To our surprise, different lots of BSA-FV varied in the ability to accelerate HSC-mediated blood system reconstitution (Figure 1B), and did not correlate with colony formation. Culture in BSA-FV #1 resulted in peripheral blood (PB) chimerism (at 12 weeks after the transplantation) of more than 50%, while BSA-FV #15 cultured cells were essentially undetectable. We hypothesized that these results were due to different compositions of unknown factors in each lot of BSA-FV.



To test this hypothesis, we attempted to detect the presence of unknown factors in BSA-FV using SDS-PAGE analysis. In addition to the major albumin protein, a number of unidentified bands were detected in BSA-FV #1, #8, and #15 (Figures 1C and 1D). Interestingly, in agreement with lot-to-lot variability in band patterns, further high-performance liquid chromatography-mass spectrometry (HPLC-MS) analysis revealed that different lots of BSA-FV exhibit distinct protein profiles (Figure 1E and Table S1). These results suggest that differences in HSC maintenance can be ascribed to varying levels of unidentified proteins contained in BSA-FV.

HSC Maintenance Varies Depending on Different Lots of BSA-FV

To assess the ability of BSA-FV to augment cytokine-mediated HSC maintenance, we cultured 40 CD34⁺KSL cells in the presence of 1% BSA-FV, SCF, TPO, and 30 different individual ligands. These 30 ligands were selected based on the expression of their receptors on CD34⁺ HSCs, identified from a previously published DNA microarray expression dataset. After 1 week, cultured cells were then transplanted into lethally irradiated recipient mice along with competitor cells and the ratio of PB chimerism determined 12 weeks after transplantation. To our surprise, the effect of each cytokine on the maintenance of HSCs changed dramatically when different BSA-FV lots were used. For instance, although IL-11 was reported to promote the growth of primitive hematopoietic progenitors in cooperation with IL-4 (Jacobsen et al., 1995), the ratio of chimerism induced by IL-11 was higher than that of control when BSA-FV #1 was used (Figure 2A), but the opposite result was obtained for BSA-FV #8 (Figure 2B). In addition, PB chimerism was detected in the presence of epidermal growth factor, insulin-like growth factor 2, or platelet-derived growth factor (PDGF) when BSA-FV #1 was used, whereas we could not observe any PB chimerism under the same conditions when BSA-FV #8 was used. From the viewpoint of reproducibility, these results suggest that simple addition of BSA-FV to cell culture should be reconsidered for efficient *in vitro* maintenance of HSCs. To further confirm these results, we repeated the same experiment focusing on IL-1 α , CXCL10, IL-4, and IL-11. The results clearly demonstrated that, as was the case for IL-1 α , the effect of the cytokine on the ratio of PB chimerism depended on the BSA-FV lot (Figures 2C and 2D).

Recombinant Protein-Based Culture Is a Promising Standard Culture System for HSC Maintenance and Expansion

To improve reproducibility in HSC proliferation, we established a standard BSA-FV free HSC culture system. After trial and error, we focused on a purified recombinant serum

albumin (RSA). We first analyzed the effect of four different RSAs on HSC maintenance and the ratio of chimerism (Figure 3A). Although RSA produced by rice (#C and #D) did not show any effect, RSA produced by yeast (#A and #B) exhibited repopulation ability and multi-lineage output (Figure S1A), regardless of lot or manufacturer. Furthermore, human RSA (HSA) and mouse RSA (MSA) produced by yeast equally maintained HSC reconstitution ability and multi-lineage output (Figures 3B and S1B). These results indicate that culture conditions containing RSA could be a promising candidate for recombinant protein-based culture systems.

To assess the ability of HSC to proliferate in RSA cultures, we compared single HSC growth in RSA- and BSA-FV #8-based cultures. RSA-cultured HSCs exhibited growth kinetics equivalent to those cultured in BSA-FV #8 (Figure 3C). HSCs were also cultured with RSA for 1 week, and tested for their potential to reconstitute the blood system. We found that the ratio of PB chimerism after the transplantation was lower than that of BSA-FV #1, but similar to that of BSA-FV #8 (Figure 3D). RSA-, as well as BSA-FV #1- and #8-cultured HSCs, all displayed increased PB chimerism following transplantation over freshly isolated CD34⁺KSL HSCs (Figure 3D). A 7-day culture with RSA increased PB chimerism by approximately 2-fold.

Using the above recombinant protein-based culture system, we reassessed the effect of the 30 ligands to maintain HSCs *ex vivo*. These experiments identified several factors that increased the ratio of PB chimerism at 12 weeks after transplantation (Figure 3E). These results were distinct from the BSA-FV-based cultures, highlighting the BSA-mediated augmentation of ligand effects. Among these 30 ligands we focused on IL-1 α , which exhibited highly elevated reconstitution ability when added to the RSA-based culture. IL-1 α has been previously reported to suppress colony formation of mouse KSL cells (Yonemura et al., 1996). However, competitive repopulation assays after *in vitro* culture showed a significantly higher ratio of PB chimerism compared with controls (Figures S2A and S2B). In addition, 16 weeks after transplantation we performed secondary transplantation and found that IL-1 α exhibits much higher levels of chimerism than controls (Figure S2C). As IL-1 α did not alter the proliferation kinetics of HSCs *in vitro* (Figure S2D), these findings strongly suggest that IL-1 α is a *bona fide* HSC maintenance factor.

Hemopexin Contained in BSA-FV Is Responsible for HSC Maintenance

HSC maintenance factors may not necessarily be ligands of receptors expressed on HSCs. As shown in Figure 1E, HPLC-MS analysis of BSA-FV #1, #8, and #15 revealed distinct protein profiles. Integrating these protein profiles with the HSC repopulation assay data allowed us to shortlist

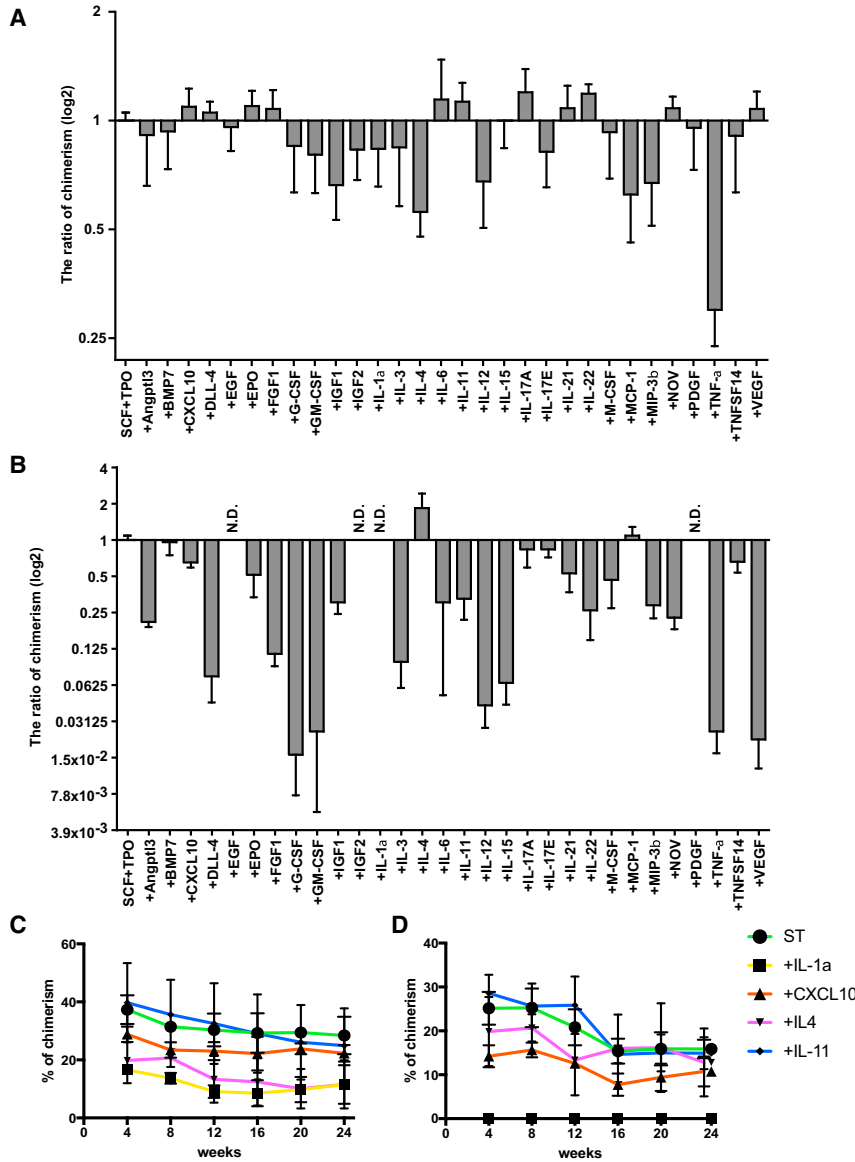


Figure 2. The Ratio of Peripheral Blood Chimerism Depends on BSA-FV Lot

(A and B) Percentage PB chimerism from 40 CD34⁺ KSL HSCs cultured for 1 week in the presence of 30 different cytokines, SCF, TPO, and BSA-FV #1 (A) or #8 (B), and transplanted into lethally irradiated recipient mice together with 10⁶ BM competitor cells. PB chimerism at 12 weeks after transplantation (n = 5 mice per BSA-FV culture condition). Mean \pm SD from two independent experiments, calculated as a ratio relative to SCF + TPO only conditions.

(C and D) As above, but displayed as percentage PB chimerism for selected cytokines (IL-1 α , CXCL10, IL-4, IL-11) cultured with 1% BSA-FV #1 (C) or #8 (D) between 4 and 24 weeks post transplantation.

putative HSC maintenance factors for investigation with a recombinant protein-based culture system. To determine the functional significance of these factors, we prepared recombinant proteins and assessed their effect on HSC repopulating ability by competitive repopulation assays following 1 week of culture with or without each recombinant protein.

One factor tested by this system, HPX, significantly increased levels of PB chimerism when added to the in vitro HSC culture in both primary and secondary transplantation recipients (Figures 4A, 4B, and S3A). Further studies demonstrated that as little as 5 ng/mL HPX could induce this increase in HSC repopulating ability (Figure S3B). To assess whether HPX is present in other lots of BSA-FV, we analyzed HPX levels in different lots of

BSA-FV by western blotting, and found that three out of eight BSA-FV lots (#A, #B, and #H) contained a significant amount of HPX (Figure 4C). Consistent with this observation, competitive repopulation assays clearly demonstrated that HSCs cultured with HPX-positive BSA-FV exhibited higher chimerism than HPX-negative controls (Figure 4D).

HPX is a heme-binding plasma glycoprotein (Muller-Eberhard, 1988) that prevents heme-mediated oxidative stress (Tolosano and Altruda, 2002). Given the described negative effects of ROS on HSC function, we hypothesized that HPX enhances HSC function through inhibiting oxidative stress. We therefore evaluated the in vitro effect of HPX on ROS production in HSCs (Figure S3C). Consistent with our hypothesis, we observed a significant reduction of ROS activity in HSCs cultured with HPX, compared

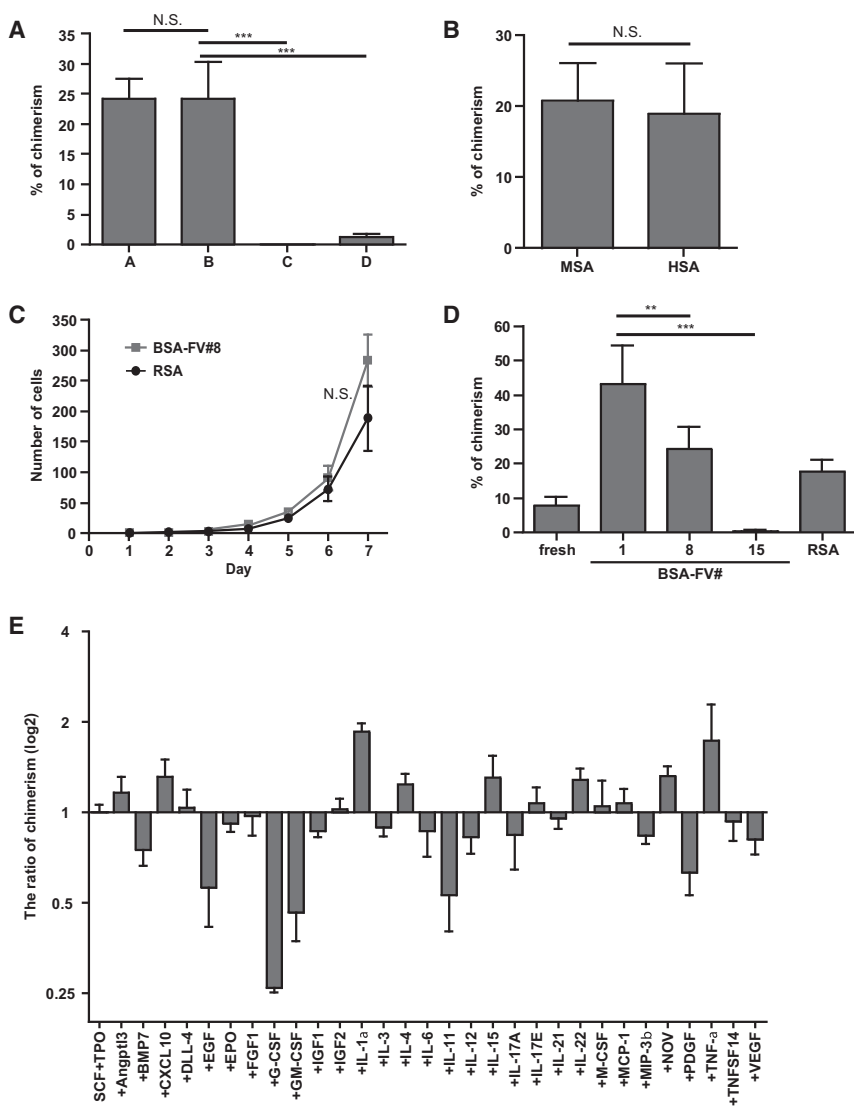


Figure 3. Recombinant Serum Albumin Can Replace BSA-FV for Ex Vivo Culture of HSCs

(A) Percentage PB chimerism from 40 CD34⁻KSL cells, following 1 week of culture with cytokines and 1% RSA produced by either yeast (A and B) and rice (C and D). PB chimerism 12 weeks after transplantation into lethally irradiated recipients together with 10⁶ BM competitor cells (n = 8 mice per RSA culture condition). Mean ± SD from two independent experiments.

(B) As in (A) but cultured with 1% MSA or HSA. Mean ± SD from three independent experiments (n = 8 mice per RSA culture condition).

(C) Single CD34⁻KSL HSCs were cultured for 1 week in 96-well microtiter plates in S-Clone SF-03 supplemented with SCF, TPO, and 1% BSA-FV #8 (gray line) or RSA (black line). Cell numbers were counted every 24 hr under a microscope. Mean ± SEM (n = 40 per RSA culture condition).

(D) As in (A) but for either freshly isolated HSCs cultured for 7 days with 1% BSA-FV #1, #8, #15, or RSA. Mean ± SD from two independent experiments (n = 10 mice per RSA culture condition).

(E) Percentage PB chimerism of 40 CD34⁻KSL HSCs (cultured for 1 week in the presence of different cytokines, SCF, TPO, and RSA) 12 weeks after transplantation into lethally irradiated recipient mice together with 10⁶ BM competitor cells. Mean ± SD from two independent experiments (n = 5 mice per cytokine culture condition), calculated as a ratio relative to SCF + TPO only conditions. Statistical significance denoted by **p < 0.05, ***p < 0.005, or N.S. (not significant) as determined by unpaired t test.

with control cultured HSCs (Figure 4E). HPX did not alter HSC proliferation kinetics in vitro (Figure S3D), highlighting that HPX enhances HSC maintenance rather than cell proliferation.

HPX expression has previously been reported in liver, CNS, retina, and peripheral nerves (Chen et al., 1998; Swerts et al., 1992; Tolosano et al., 1996). Given that peripheral nerves include non-myelinating Schwann cells, which are also a constituent of HSC niche (Yamazaki et al., 2011), we were interested in whether this BM cell type also expressed HPX. We therefore investigated HPX expression by immunostaining BM sections along with glial fibrillary acidic protein (GFAP) expression, and confirmed overlapping expression of HPX and GFAP in all sections (Figures 4F and 4G). Furthermore, using a

recently developed whole-body imaging by tissue decolorization technique, we performed 3D immunohistochemistry of whole BM and further confirmed co-localization of HPX and GFAP (Figure 4H and Movie S1). While the majority of HPX co-localized with GFAP, HPX staining was also seen elsewhere within the BM, suggesting that other BM niche cells express HPX. These results raise the intriguing possibility that HPX protects HSCs from oxidative stress in specialized BM niches, although further work is necessary to define the role of HPX in vivo.

Finally, we attempted to quantitate the effects of HPX and IL-1 α on in vitro HSC maintenance and expansion using limiting dilution analysis by transplanting 1,000, 100, and 10 cells (following a 7-day culture) alongside 2 × 10⁵ BM competitors. Surprisingly, all mice displayed significant

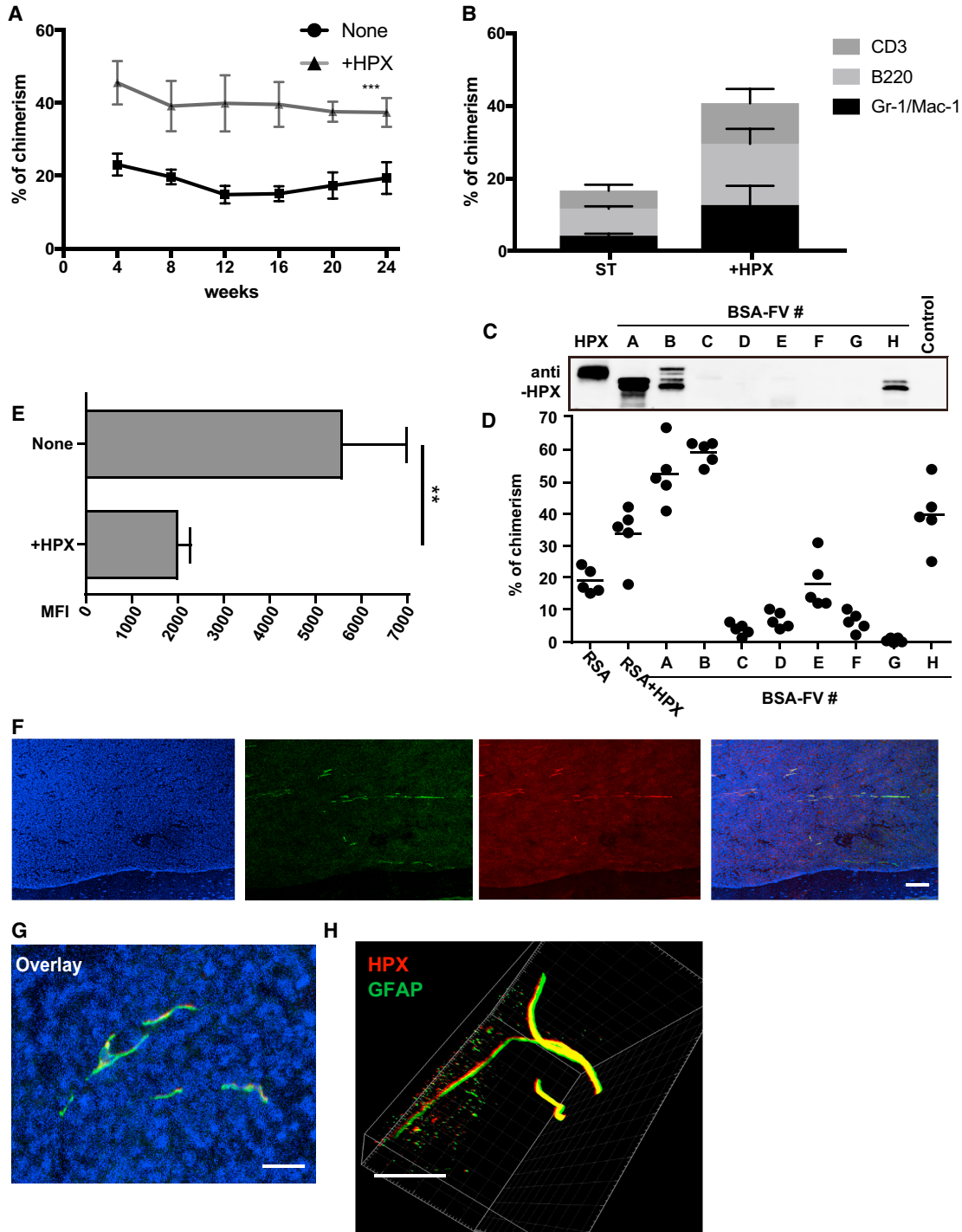


Figure 4. The All-Recombinant Protein-Based Culture System Contributes to Identification of HSC Maintenance Factors Contained in BSA-FV

(A and B) The percentage PB chimerism from 40 CD34⁻KSL HSCs following culture for 1 week in the presence SCF, TPO, RSA, and with or without HPX (10 ng/mL) before transplantation into lethally irradiated recipient mice together with 10⁶ BM competitor cells. PB chimerism measured over 24 weeks post transplantation (n = 4 or 5 mice per culture condition) and displayed as total PB chimerism (A) and blood-lineage chimerism (B) within the myeloid (Gr-1/Mac-1⁺), B cell (B220⁺), and T cell (CD3⁺) lineages at 12 weeks. Mean ± SD from two independent experiments.

(legend continued on next page)



donor cell chimerism (>90% in some mice) within the PB after 4 weeks (Figure S4). While these results precluded quantitation of HSC frequency, they do highlight the ability of RSA-based cultures to expand blood system reconstituting cells in vitro. After all, single HSCs on average give rise to approximately 200 progenies during the 7-day RSA culture (Figure 3C), yet substantial PB chimerism was detected from aliquots of 100 and 10 HSC progenies (1/2 and 1/20 HSC equivalents, respectively).

DISCUSSION

Reproducibility is of central importance in experimental science. Unfortunately, in the case of in vitro maintenance of HSCs, reproducible results are often not obtained. Several factors are likely responsible, including the variability of culture reagents, insufficient culture conditions, and (im) purity of phenotypic HSCs. Data presented here highlight the wide variety of in vitro HSC maintenance capabilities of different BSA-FV preparations. To overcome these limitations, we have developed a fully defined all-recombinant protein-based system for the in vitro culture of murine HSCs. Using this system, we have demonstrated that IL-1 α and HPX, often contained within BSA-FV, significantly enhance in vitro maintenance of HSCs. This system therefore provides a basis on which to develop a reproducible in vitro HSC maintenance and expansion culture system.

Development of stable in vitro expansion conditions for HSCs would have important implications for both basic research and clinical use. In particular, stable ex vivo expansion of HSCs would reduce current shortages in donors for clinical BM transplantation and could afford ex vivo gene correction approaches for inherited hematological disorders. Furthermore, recent efforts to generate HSCs in vitro by directed differentiation and reprogramming are currently limited by our inability to maintain any HSCs generated in vitro. Here, we propose an all-recombinant protein-based system with which to develop such culture conditions, and systematic approaches by which to develop optimal conditions.

Based on DNA microarray data, we tested the functions of 30 different candidate factors by adding them one

by one to HSC culture medium. Consequently, we were able to identify two HSC maintenance factors, IL-1 α and HPX. In previous studies, IL-1 α was reported to support the proliferation of mouse HSCs in cooperation with IL-3 (Jubinsky and Stanley, 1985; Mochizuki et al., 1987), while another group reported that the same factor reduces the colony-forming and reconstitution ability of HSCs (Yonemura et al., 1996). These contradictory results highlight the problems of using variable reagents such as conditioned medium or FBS. In the present study, we were able to reveal that IL-1 α in fact contributes to the PB reconstitution potential of HSCs (Figures S1A and S1B). However, we note that high concentrations of IL-1 α (100 ng/mL) inhibited colony formation (data not shown).

Furthermore, we were able to identify HPX as an HSC maintenance factor contained within BSA-FV. HPX is thought to inhibit heme-induced ROS generation. While hematopoietic defects in HPX knockout mice have not been described (Tolosano et al., 1999), our results demonstrated that HPX reduced ROS level of cultured HSCs and improved their reconstitution capability. HPX is unlikely to be the only HSC maintenance factor in BSA-FV, and we believe that protein profiling of “good” BSA-FV batches, as described here, will allow further identification of novel HSC maintenance and expansion factors.

In conclusion, we believe that the all-recombinant protein-based system described here is an exciting research tool for generating highly robust and reproducible data, and one that will provide important contributions in our efforts to identify growth and differentiation factors for HSCs, as well as many other different stem cell populations.

EXPERIMENTAL PROCEDURES

HSC Purification

Mouse CD34⁺KSL HSCs were purified from BM cells of 8- to 10-week-old mice. See Supplemental Experimental Procedures for a detailed description.

HSC Culture

CD34⁺KSL HSCs were deposited into 96-well microtiter plates containing 200 μ L of serum-free medium S-Clone SF-03 (Sanko

(C) Immunoblotting for HPX of albumin-depleted BSA-FV.

(D) Lethally irradiated recipient mice were transplanted with 10⁶ BM competitor cells and 40 CD34⁺KSL HSCs cultured for 1 week with 1% BSA-FV or 1% RSA with or without HPX (all in the presence of SCF and TPO). Percentage PB chimerism at 12 weeks post transplantation (n = 5 mice per BSA-FV culture condition). Mean \pm SD of three independent experiments.

(E) Effect of HPX on ROS levels of in vitro cultured HSCs, as measured by flow cytometric analysis of HySOx staining. Mean fluorescence intensity (MFI) values \pm SD (n = 5 per culture condition).

(F and G) Fluorescence imaging of BM sections co-stained with anti-HPX (red), anti-GFAP (green), and DAPI (blue) antibodies. Scale bars: (F) 100 μ m; (G) 4 μ m.

(H) 3D fluorescence image of a representative tibia BM, stained with anti-HPX (red) and anti-GFAP (green). Scale bar, 150 μ m.

Statistical significance denoted by **p < 0.05 and ***p < 0.005 as determined by unpaired t test.



Junyaku) supplemented with 1% BSA (Sigma and Wako), MSA, or HSA (Albumin Bioscience, Sigma, Bioverde) and cytokines (50 ng/mL mouse SCF, 50 ng/mL human TPO).

Competitive Repopulation Assays

Competitive repopulation assays were performed using the Ly5 congenic mouse system. Forty CD34⁺KSL cells from B6-Ly5.1 and the BM competitor cells (1×10^6) from B6-F1 mice were transplanted into B6-Ly5.2 mice irradiated at a dose of 9.8 Gy. See [Supplemental Experimental Procedures](#) for a detailed description.

Sample Purification for Mass Spectrometry

Depletion of albumin from BSA-FV was performed using Melon Gel IgG Spin Purification Kit (Thermo Scientific) according to the manufacturer's instructions.

BM Immunofluorescence and 3D Imaging

Frozen BM sections were prepared and immunostained according to the Kawamoto method ([Kawamoto, 2003](#)). 3D imaging was performed as previously described ([Susaki et al., 2015](#)).

SUPPLEMENTAL INFORMATION

Supplemental Information includes Supplemental Experimental Procedures, four figures, one table, and one movie and can be found with this article online at <http://dx.doi.org/10.1016/j.stemcr.2017.01.015>.

AUTHOR CONTRIBUTIONS

A.I., I.R., T.K., and S.Y. planned and performed the experiments and wrote the manuscript. M.M. helped perform experiments. A.W., K.S., T.N., J.O., Y.T., C.L., M.O., Y.N., H.E., and H.N. provided scientific discussion and technical support. H.E. provided scientific discussion. S.Y., A.W., and H.N. directed the study and wrote the manuscript.

ACKNOWLEDGMENTS

We thank Drs. R. Yamamoto, Ishii, Y. Yamazaki, and A Tojo for technical help and advice, and Dr. M. Kasai for critical reading of the manuscript. This work was supported by grants from Japan Science and Technology Agency (JST) (grant no. 50625580), the Ministry of Education, Culture, Sport, Science, and Technology (Japan), California Institute of Regenerative Medicine (grant no. LA1-06917), Siebel Foundation, and Ludwig Foundation.

Received: July 27, 2016

Revised: January 17, 2017

Accepted: January 18, 2017

Published: February 23, 2017

REFERENCES

Barker, J.E. (1994). Sl/Slid hematopoietic progenitors are deficient in situ. *Exp. Hematol.* *22*, 174–177.

Calvi, L.M., Adams, G.B., Weibrecht, K.W., Weber, J.M., Olson, D.P., Knight, M.C., Martin, R.P., Schipani, E., Divieti, P., Bringhurst,

F.R., et al. (2003). Osteoblastic cells regulate the haematopoietic stem cell niche. *Nature* *425*, 841–846.

Chen, W., Lu, H., Dutt, K., Smith, A., Hunt, D.M., and Hunt, R.C. (1998). Expression of the protective proteins hemopexin and haptoglobin by cells of the neural retina. *Exp. Eye Res.* *67*, 83–93.

Eaves, C.J. (2015). Hematopoietic stem cells: concepts, definitions, and the new reality. *Blood* *125*, 2605–2613.

Guilbert, L.J., and Iscove, N.N. (1976). Partial replacement of serum by selenite, transferrin, albumin and lecithin in haemopoietic cell cultures. *Nature* *263*, 594–595.

Iwama, A., Oguro, H., Negishi, M., Kato, Y., Morita, Y., Tsukui, H., Ema, H., Kamijo, T., Katoh-Fukui, Y., Koseki, H., et al. (2004). Enhanced self-renewal of hematopoietic stem cells mediated by the polycomb gene product Bmi-1. *Immunity* *21*, 843–851.

Jacobsen, F.W., Keller, J.R., Ruscetti, F.W., Veiby, O.P., and Jacobsen, S.E. (1995). Direct synergistic effects of IL-4 and IL-11 on proliferation of primitive hematopoietic progenitor cells. *Exp. Hematol.* *23*, 990–995.

Jubinsky, P.T., and Stanley, E.R. (1985). Purification of hemopoietin 1: a multilineage hemopoietic growth factor. *Proc. Natl. Acad. Sci. USA* *82*, 2764–2768.

Kawamoto, T. (2003). Use of a new adhesive film for the preparation of multi-purpose fresh-frozen sections from hard tissues, whole-animals, insects and plants. *Arch. Histol. Cytol.* *66*, 123–143.

Kiel, M.J., and Morrison, S.J. (2008). Uncertainty in the niches that maintain haematopoietic stem cells. *Nat. Rev. Immunol.* *8*, 290–301.

Kiel, M.J., Yilmaz, O.H., Iwashita, T., Terhorst, C., and Morrison, S.J. (2005). SLAM family receptors distinguish hematopoietic stem and progenitor cells and reveal endothelial niches for stem cells. *Cell* *121*, 1109–1121.

Ku, H., Yonemura, Y., Kaushansky, K., and Ogawa, M. (1996). Thrombopoietin, the ligand for the Mpl receptor, synergizes with steel factor and other early acting cytokines in supporting proliferation of primitive hematopoietic progenitors of mice. *Blood* *87*, 4544–4551.

Mendez-Ferrer, S., Michurina, T.V., Ferraro, F., Mazloom, A.R., MacArthur, B.D., Lira, S.A., Scadden, D.T., Ma'ayan, A., Enikolopov, G.N., and Frenette, P.S. (2010). Mesenchymal and haematopoietic stem cells form a unique bone marrow niche. *Nature* *466*, 829–834.

Mochizuki, D.Y., Eisenman, J.R., Conlon, P.J., Larsen, A.D., and Tushinski, R.J. (1987). Interleukin 1 regulates hematopoietic activity, a role previously ascribed to hemopoietin 1. *Proc. Natl. Acad. Sci. USA* *84*, 5267–5271.

Muller-Eberhard, U. (1988). Hemopexin. *Methods Enzymol.* *163*, 536–565.

Osawa, M., Hanada, K., Hamada, H., and Nakauchi, H. (1996). Long-term lymphohematopoietic reconstitution by a single CD34-low/negative hematopoietic stem cell. *Science* *273*, 242–245.

Sauvageau, G., Thorsteinsdottir, U., Eaves, C.J., Lawrence, H.J., Largman, C., Lansdorp, P.M., and Humphries, R.K. (1995). Overexpression of HOXB4 in hematopoietic cells causes the selective expansion of more primitive populations in vitro and in vivo. *Genes Dev.* *9*, 1753–1765.



- Sugiyama, T., Kohara, H., Noda, M., and Nagasawa, T. (2006). Maintenance of the hematopoietic stem cell pool by CXCL12-CXCR4 chemokine signaling in bone marrow stromal cell niches. *Immunity* 25, 977–988.
- Susaki, E.A., Tainaka, K., Perrin, D., Yukinaga, H., Kuno, A., and Ueda, H.R. (2015). Advanced CUBIC protocols for whole-brain and whole-body clearing and imaging. *Nat. Protoc.* 10, 1709–1727.
- Swerts, J.P., Soula, C., Sagot, Y., Guinaudy, M.J., Guillemot, J.C., Ferrara, P., Duprat, A.M., and Cochard, P. (1992). Hemopexin is synthesized in peripheral nerves but not in central nervous system and accumulates after axotomy. *J. Biol. Chem.* 267, 10596–10600.
- Tolosano, E., and Altruda, F. (2002). Hemopexin: structure, function, and regulation. *DNA Cell Biol.* 21, 297–306.
- Tolosano, E., Cutufia, M.A., Hirsch, E., Silengo, L., and Altruda, F. (1996). Specific expression in brain and liver driven by the hemopexin promoter in transgenic mice. *Biochem. Biophys. Res. Commun.* 218, 694–703.
- Tolosano, E., Hirsch, E., Patrucco, E., Camaschella, C., Navone, R., Silengo, L., and Altruda, F. (1999). Defective recovery and severe renal damage after acute hemolysis in hemopexin-deficient mice. *Blood* 94, 3906–3914.
- Walasek, M.A., van Os, R., and de Haan, G. (2012). Hematopoietic stem cell expansion: challenges and opportunities. *Ann. N. Y. Acad. Sci.* 1266, 138–150.
- Yamazaki, S., Iwama, A., Takayanagi, S., Morita, Y., Eto, K., Ema, H., and Nakauchi, H. (2006). Cytokine signals modulated via lipid rafts mimic niche signals and induce hibernation in hematopoietic stem cells. *EMBO J.* 25, 3515–3523.
- Yamazaki, S., Ema, H., Karlsson, G., Yamaguchi, T., Miyoshi, H., Shioda, S., Taketo, M.M., Karlsson, S., Iwama, A., and Nakauchi, H. (2011). Nonmyelinating Schwann cells maintain hematopoietic stem cell hibernation in the bone marrow niche. *Cell* 147, 1146–1158.
- Yonemura, Y., Ku, H., Hirayama, F., Souza, L.M., and Ogawa, M. (1996). Interleukin 3 or interleukin 1 abrogates the reconstituting ability of hematopoietic stem cells. *Proc. Natl. Acad. Sci. USA* 93, 4040–4044.
- Zhang, J., Niu, C., Ye, L., Huang, H., He, X., Tong, W.G., Ross, J., Haug, J., Johnson, T., Feng, J.Q., et al. (2003). Identification of the haematopoietic stem cell niche and control of the niche size. *Nature* 425, 836–841.

Stem Cell Reports, Volume 8

Supplemental Information

An All-Recombinant Protein-Based Culture System Specifically Identifies Hematopoietic Stem Cell Maintenance Factors

Aki Ieyasu, Reiko Ishida, Takaharu Kimura, Maiko Morita, Adam C. Wilkinson, Kazuhiro Sudo, Toshinobu Nishimura, Jun Ohehara, Yoko Tajima, Chen-Yi Lai, Makoto Otsu, Yukio Nakamura, Hideo Ema, Hiromitsu Nakauchi, and Satoshi Yamazaki

Supplementary Experimental Procedures

Mice

C57BL/6 (B6-Ly5.2) mice were purchased from SLC (Shizuoka, Japan) and B6-Ly5.1 from Sankyo Lab Service (Tsukuba, Japan). All animal care was in accordance with the guidelines of the University of Tokyo.

Purification of murine hematopoietic stem cells

Mouse CD34⁻KSL HSCs were purified from BM cells of 8 to 10 week-old mice. Whole bone marrow cells were stained with an antibody cocktail consisting of biotinylated anti-Gr-1 (#13593185), -Mac-1 (#13011285), -CD4 (#13004285), -IL-7R (13127185), and -Ter-119 (#13592185) (eBioscience, San Diego, CA), and -B220 (#13045285) and -CD8 (#13008185) monoclonal antibodies (BioLegend, San Diego, CA) (lineage cocktail). Lineage-positive cells were depleted with anti-Biotin MicroBeads (MiltenyiBiotec, Auburn, CA) using LS columns (MiltenyiBiotec). The lineage-depleted fraction was then further stained with fluorescein isothiocyanate (FITC)-conjugated anti-CD34 (#11034185, BD Bioscience, California, CA), phycoerythrin (PE)-conjugated anti-Sca-1 (#108108, eBioscience), and allophycocyanin (APC)-conjugated anti-c-Kit antibodies (#17117183, BioLegend). Biotinylated antibodies were detected with streptavidin-APC-Cy7 (#47431782, BioLegend). Analysis and cell sorting were performed on a FACS Aria (BD Bioscience) and results were analyzed with FlowJo software (Tree Star, Ashland, OR).

Hematopoietic stem cell culture system

CD34⁻KSL HSCs were deposited into 96-well micro-titer plates containing 200 μ l of serum free medium S-Clone SF-03 (Sanko JunyakuInc, Tokyo, Japan) supplemented with 1% BSA (Sigma, and Wako, Japan), MSA or HSA (Albumin Bioscience, Sigma, Bioverde) and cytokines (50 ng/ml mouse SCF, 50 ng/ml human TPO).

Competitive repopulation assays

40 CD34⁺KSL cells from B6-Ly5.1 and the BM competitor cells (1×10^6) from B6-F1 mice were transplanted into B6-Ly5.2 mice irradiated at a dose of 9.8 Gy. Following transplantation, peripheral blood (PB) cells of the recipients were stained with PE-conjugated anti-Ly5.1 (BioLegend) and FITC-conjugated anti-Ly5.2 (BD Bioscience). The cells were further stained with PE-Cy7-conjugated anti-Mac-1 and -Gr-1, Pacific Blue (PB)-conjugated anti-B220 and APC-Cy7-conjugated anti-CD3 antibodies (BioLegend) and analyzed using a FACS Aria. Secondary BM transplantation assays were performed by transferring 1×10^6 BM cells from the primary recipient mice into lethally irradiated B6-Ly5.2 mice. PB cells were collected from secondary recipient mice at 4, 8, 12 and 16 weeks post-transplantation and analyzed as above. For limiting dilution assays, 1000, 100, and 10 (seven-day) cultured cells were aliquoted by FACS and transplantation into lethally-irradiated mice together with 2×10^5 BM competitor cells. PB cells were collected at 4 weeks post-transplantation and analyzed as above.

Purification samples for Mass Spectrometry analysis

Depletion of albumin from BSA-FV was performed using Melon Gel IgG Spin Purification Kit (Thermo Scientific) according to the manufacturer's instructions. Briefly, 500 μ l of 10% BSA-FV in 10 mM HEPES pH7.3 was diluted 1:10 in Melon Gel Purification Buffer and applied to Melon Gel spin columns. After incubation for 5 min at room temperature with rotation, spin columns were centrifuged and flow through was used for mass spectrometry analysis (Medical & Biological Laboratories CO., LTD.).

Western blotting

500 μ g of BSA-FV was subjected to albumin depletion. Total flow-through of Melon Gel was applied to SDS-PAGE, transferred to PVDF membranes and blots were incubated with rabbit polyclonal anti-hemopexin antibody (#ab133415, 1:1000, Abcam) for 30 min at room temperature. Following incubation with an appropriate secondary antibody, immunoreactivity was detected by chemiluminescence using Image Quant LAS4000 (GE Healthcare Life Science).

ROS detection assay

CD34⁺KSL cells were collected after 2 days of culture and stained with HySOx (excitation: 555 nm, emission: 575 nm; Goryo Chemical, Hokkaido, Japan), for 30 minutes at 37°C. After washing, cells were analyzed for ROS accumulation by FACS Aria. Cellular ROS were quantified by mean fluorescence intensity (MFI).

Immunofluorescence staining of BM sections

Frozen BM sections were prepared and immunostained according to the Kawamoto method (Kawamoto, 2003). BM sections were fixed using dry ice/ethanol or 4% paraformaldehyde (PFA). Immunofluorescence data were obtained and analyzed with a TCS SP2 AOBS confocal microscope (Leica, Microsystems, Tokyo). The immunofluorescence-microscopy images of BM sections were automatically obtained, using integrated reader software, from multiple replicates. Markers and antibodies used were: Alexa 488-conjugated goat anti-Rabbit IgG, and Alexa 647-conjugated goat anti-rabbit IgG (Molecular Probes, Carlsbad, CA, USA); rabbit anti-GFAP (#Z0334, Dako, Glostrup, Denmark); sheep anti-hemopexin (#MAB7007, R&D systems); 4, 6-diamidino-2-phenylindole (DAPI), a DNA marker.

3D imaging

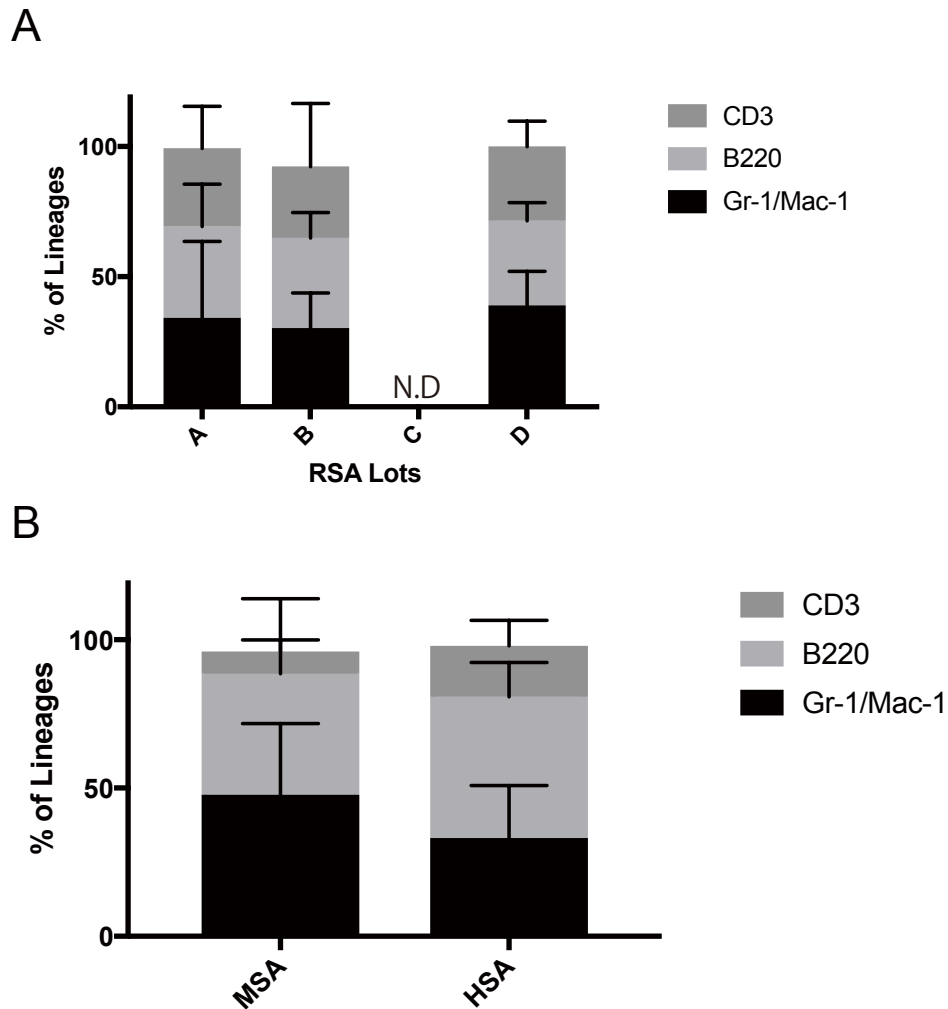
3D imaging was performed as previously described (Susaki et al., 2015). In brief, after tibias were collected and fixed in 4% PFA solution, bone marrow plugs were extracted from bones by flushing. Upon DAPI staining, marrow plugs were treated with ScaleCUBIC-1 (Reagent-1) for one week followed by ScaleCUBIC-2 (Reagent-2) for another week. To visualize GFAP⁺ cells and hemopexin⁺ cells were stained overnight with antibodies. Images were acquired using a ZEISS Z1 Lightsheet microscope (ZEISS) and 3D reconstitutions were performed with Imaris software (Bitplane).

Statistical analysis

Mean values of two groups were compared using two-tail unpaired t testing. All statistical analyses were performed on Prism 7 software (Graphpad, San Diego, CA).

Supplemental Figure and Figure Legends

Supplemental Figure 1

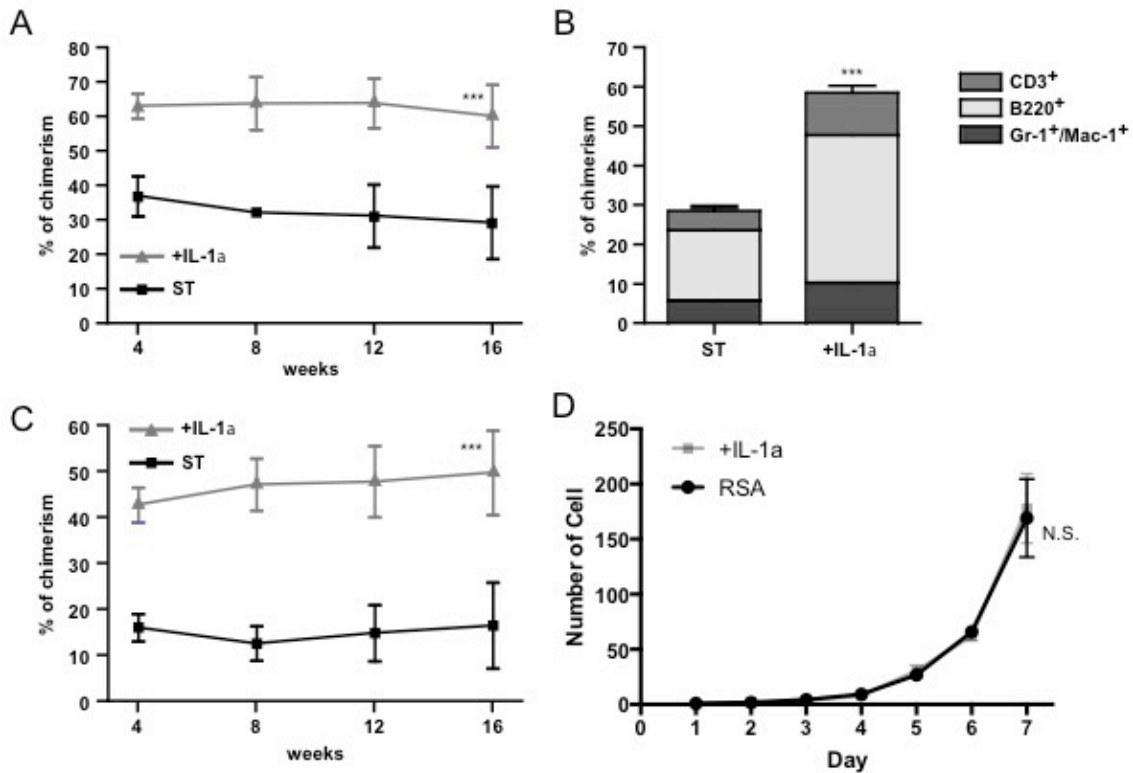


Supplementary Figure 1: Multi-lineage HSC output following RSA-based culture

(A) Ratio of myeloid (Gr-1/Mac-1⁺), B cell (B220⁺) and T cell (CD3⁺) PB chimerism from 40 CD34-HSCs cultured for seven days in various lots of RSA (A-D) supplemented with SCF and TPO. Mean ratios \pm SDs at 12 weeks post-transplantation, as described in Figure 3A (n = 5 per BSA-FV culture condition).

(B) Ratio of myeloid (Gr-1/Mac-1⁺), B cell (B220⁺) and T cell (CD3⁺) PB chimerism from 40 CD34-HSCs cultured for seven days in mouse RSA (MSA) or human RSA (HSA) supplemented with SCF and TPO. Mean ratios \pm SDs at 12 weeks post-transplantation, as described in Figure 3B (n = 5 per RSA culture condition).

Supplemental Figure 2



Supplementary Figure 2: IL-1 α enhances *in vitro* HSC maintenance

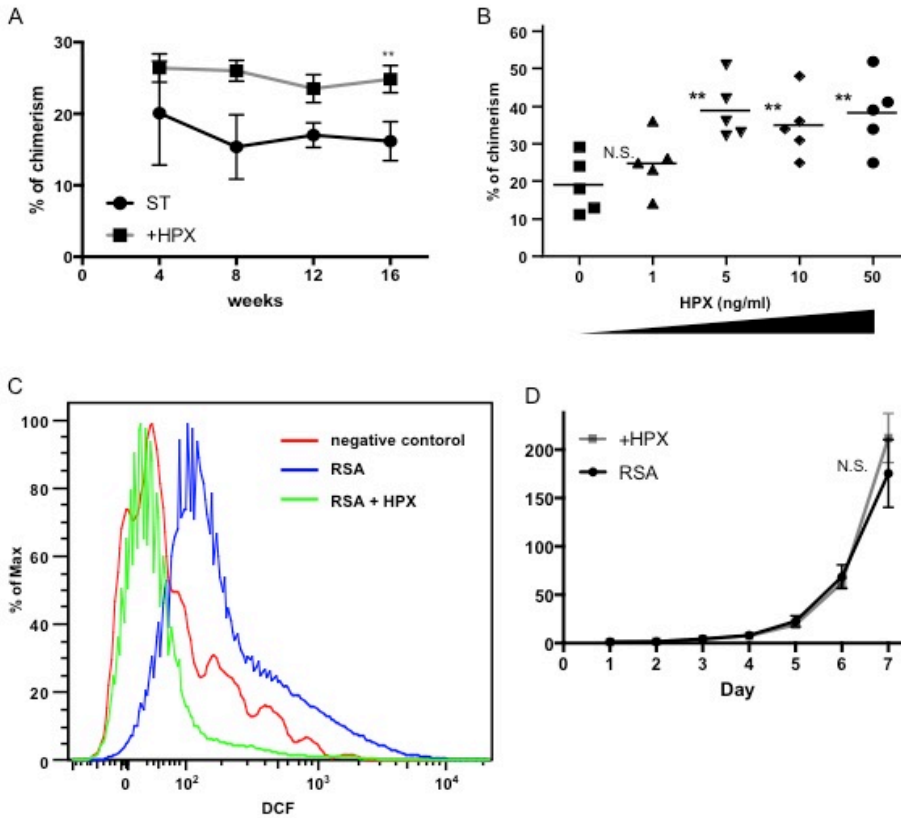
(A,B) 40 CD34⁺KSL HSCs were cultured for one week with 1% HSA, SCF, TPO and 20 ng/ml IL-1 α before transplantation into lethally irradiated mice together with 10⁶ BM competitor cells. (A) Time course analysis of PB chimerism. (B) The donor-derived PB cell ratio 12 weeks after transplantation. The data presented are the mean ratios \pm SDs of two independent experiments (n = 5 per culture condition).

(C) Secondary competitive repopulation analysis of BM from mice in (A). Data are the mean \pm SD of donor-derived PB cells (n = 10 per culture condition).

(D) Proliferation of HSCs with RSA with IL-1 α *in vitro*. Single CD34⁺KSL HSCs were cultured for one week in 96-well micro-titer plates in S-Clone SF-03 supplemented with SCF, TPO and 1% RSA (black line) with or without 20 ng/ml IL-1 α . Cell numbers were counted every 24 hours under a microscope. Data are the mean \pm SEM (n = 40 per culture condition).

Statistical significance denoted by ** ($P < 0.05$), *** ($P < 0.005$) or N.S. (not significant) as determined by unpaired t testing.

Supplemental Figure 3



Supplementary Figure 3: Hemopexin enhances engraftment of *in vitro* cultured HSCs

(A) Secondary competitive repopulation analysis of BM from mice in Figure 4A. Data are the mean ± SD of donor-derived PB cells (n = 10 per culture condition).

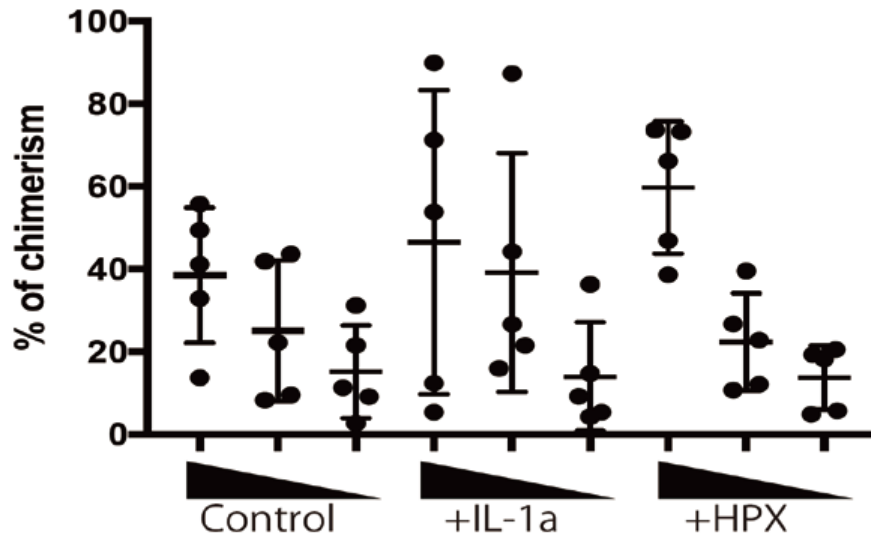
(B) 40 CD34⁺KSL cells were cultured for 1 week with 1% MSA, SCF, TPO and various concentrations of HPX before transplantation into lethally irradiated recipient mice together with 10⁶ BM competitor cells. The donor-derived chimerism was measured 12 weeks after transplantation. Data are the mean ± SD of donor-derived cells in the PB (n = 5 per culture condition) of two independent experiments.

(C) Representative flow cytometric plots displaying HySOx staining (a measure of ROS levels) of HSCs cultured *in vitro* with or without HPX.

(D) Proliferation of HSCs with RSA with HPX *in vitro*. Single CD34⁺KSL HSCs were cultured for one week in 96-well micro-titer plates in S-Clone SF-03 supplemented with SCF, TPO and 1% RSA (black line) with or without 10 ng/ml HPX. Cell numbers were counted every 24 hours under a microscope. Data are the mean ± SEM (n = 40 per culture condition).

Statistical significance denoted by ** ($P < 0.05$), *** ($P < 0.005$) or N.S. (not significant) as determined by unpaired t testing.

Supplemental Figure 4



Supplementary Figure 4: Limiting dilution analysis of RSA-cultured HSCs

40 CD34⁺KSL HSCs were cultured for one week with 1% HSA, SCF, TPO with or without 20 ng/ml IL-1 α or 10 ng/ml HPX. 1000 (left bar), 100 (middle bar) and 10 (right bar) cultured cells were then aliquoted by FACS and transplantation into lethally irradiated mice together with 2×10^5 BM competitor cells. PB chimerism at 4 weeks post-transplantation are displayed.

Supplemental Table 1

BSA-FV #1			BSA-FV #8			BSA-FV #15		
Accession number	Name	Peptides (95%)	Accession number	Name	Peptides (95%)	Accession number	Name	Peptides (95%)
gi 30794280	serum albumin precursor [Bos taurus]	1129	gi 30794280	serum albumin precursor [Bos taurus]	823	gi 30794280	serum albumin precursor [Bos taurus]	686
gi 154425704	ALB protein [Bos taurus]	971	gi 154425704	ALB protein [Bos taurus]	700	gi 74267962	ALB protein [Bos taurus]	575
gi 296490958	TPA: serotransferrin precursor [Bos taurus]	654	gi 27806789	transferrin precursor [Bos taurus]	216	gi 99028969	complement C3 preproprotein [Bos taurus]	130
gi 2501351	RecName: Full=Serotransferrin; Short=Transferrin; AltName: Full=Beta-1 metal-binding globulin; AltName: Full=Siderophilin; Flags: Precursor	636	gi 1699167	IgG2a heavy chain constant region [Bos taurus]	63	gi 27806789	transferrin precursor [Bos taurus]	92
gi 77736171	hemopexin precursor [Bos taurus]	186	gi 99028969	complement C3 preproprotein [Bos taurus]	55	gi 109939993	Apolipoprotein H (beta-2-glycoprotein I) [Bos taurus]	88
gi 114051225	protein HP-20 homolog precursor [Bos taurus]	96	gi 94966811	alpha-1-acid glycoprotein precursor [Bos taurus]	42	gi 74353860	IGL@ protein [Bos taurus]	53
gi 114050753	protein HP-25 homolog 1 precursor [Bos taurus]	55	gi 296490958	TPA: serotransferrin precursor [Bos taurus]	41	gi 151556360	Unknown (protein for MGC:159378) [Bos taurus]	51
gi 27806789	transferrin precursor [Bos taurus]	53	gi 74353860	IGL@ protein [Bos taurus]	40	gi 15088675	immunoglobulin lambda light chain [Bos taurus]	51
gi 114052108	protein HP-25 homolog 2 precursor [Bos taurus]	39	gi 296486756	TPA: complement factor I [Bos taurus]	37	gi 77735883	serum amyloid P-component precursor [Bos taurus]	49
gi 6	beta-2-glycoprotein I [Bos taurus]	37	gi 77735367	ribonuclease UK114 [Bos taurus]	36	gi 297461373	PREDICTED: complement factor H-related protein 2 [Bos taurus]	42
gi 92096965	Immunoglobulin light chain, lambda gene cluster [Bos taurus]	34	gi 108750	Ig heavy chain precursor (B/MT.4A.17.H5.A5) - bovine	28	gi 296490958	TPA: serotransferrin precursor [Bos taurus]	38
gi 116812902	hemoglobin subunit alpha [Bos taurus]	32	gi 296478893	TPA: proteoglycan 4 [Bos taurus]	24	gi 75812954	fibrinogen alpha chain precursor [Bos taurus]	16
gi 27819608	hemoglobin subunit beta [Bos taurus]	31	gi 296487872	TPA: keratin 6A [Bos taurus]	19	gi 343197018	immunoglobulin lambda light chain constant region 3 allotypic variant IGLC3b [Bos taurus]	16
gi 77735935	complement C2 precursor [Bos taurus]	30	gi 343197018	immunoglobulin lambda light chain constant region 3 allotypic variant IGLC3b [Bos taurus]	18	gi 77404252	collagen alpha-1(I) chain precursor [Bos taurus]	15
gi 91982959	immunoglobulin gamma 1 heavy chain constant region [Bos taurus]	27	gi 27807007	insulin-like growth factor-binding protein 3 precursor [Bos taurus]	16	gi 164414427	collagen alpha-1(II) chain isoform 2 precursor [Bos taurus]	14
gi 59858077	aspartate aminotransferase 1 [Bos taurus]	26	gi 297461373	PREDICTED: complement factor H-related protein 2 [Bos taurus]	15	gi 28189426	similar to ubiquitin-S27a fusion protein [Bos taurus]	12
gi 108750	Ig heavy chain precursor (B/MT.4A.17.H5.A5) - bovine	23	gi 296484341	TPA: protein AMBP precursor [Bos taurus]	14	gi 330688394	folate receptor alpha precursor [Bos taurus]	11
gi 270483766	beta-hexosaminidase subunit beta preproprotein [Bos taurus]	22	gi 153791660	extracellular matrix protein 1 precursor [Bos taurus]	12	gi 2323380	immunoglobulin light chain variable region [Bos taurus]	11
gi 95147674	complement factor B precursor [Bos taurus]	21	gi 95147674	complement factor B precursor [Bos taurus]	12	gi 27807007	insulin-like growth factor-binding protein 3 precursor [Bos taurus]	10
gi 296475479	TPA: fumarylacetoacetase [Bos taurus]	17	gi 310893435	immunoglobulin light chain [Bos taurus]	12	gi 2323402	immunoglobulin light chain variable region [Bos taurus]	10
gi 1699167	IgG2a heavy chain constant region [Bos taurus]	16	gi 75812954	fibrinogen alpha chain precursor [Bos taurus]	11	gi 95147674	complement factor B precursor [Bos taurus]	10
gi 343197026	immunoglobulin lambda light chain constant region 3 allotypic variant IGLC3c [Bos taurus]	15	gi 296476317	TPA: keratin, type I cytoskeletal 14 [Bos taurus]	10	gi 153791660	extracellular matrix protein 1 precursor [Bos taurus]	9
gi 358422418	PREDICTED: WASH complex subunit 7-like [Bos taurus]	13	gi 77736171	hemopexin precursor [Bos taurus]	10	gi 358420619	PREDICTED: complement C4-A [Bos taurus]	9
gi 156120479	fructose-bisphosphate aldolase A [Bos taurus]	12	gi 358421409	PREDICTED: keratin, type II cytoskeletal 1 [Bos taurus]	9	gi 84000165	complement factor I precursor [Bos taurus]	8
gi 27807261	acidic mammalian chitinase precursor [Bos taurus]	11	gi 114051856	keratin, type II cytoskeletal 7 [Bos taurus]	9	gi 75832056	apolipoprotein A-I preproprotein [Bos taurus]	7
gi 114051379	leucine-rich alpha-2-glycoprotein precursor [Bos taurus]	10	gi 358422499	PREDICTED: keratin, type I cytoskeletal 10-like [Bos taurus]	9	gi 296485168	TPA: serine peptidase inhibitor, Kazal type 5 [Bos taurus]	7
gi 2323386	immunoglobulin light chain variable region [Bos taurus]	10	gi 160395544	RecName: Full=Keratin, type I cytoskeletal 17; AltName: Full=Cytokeratin-17; Short=CK-17; Short=K17	9	gi 164450479	kininogen-2 isoform 1 precursor [Bos taurus]	7
gi 30038325	cathepsin C [Bos taurus]	9	gi 156120885	CD5 antigen-like precursor [Bos taurus]	8	gi 115497340	serum amyloid A protein precursor [Bos taurus]	6
gi 77735921	fructose-bisphosphate aldolase B [Bos taurus]	6	gi 358417209	PREDICTED: extracellular peptidase inhibitor-like [Bos taurus]	8	gi 255003702	fibronectin precursor [Bos taurus]	5
gi 296475228	TPA: serpin peptidase inhibitor, clade A (alpha-1 antiproteinase, antitrypsin), member 3 [Bos taurus]	6	gi 2323386	immunoglobulin light chain variable region [Bos taurus]	8	gi 8100793	insulin-like growth factor I [Bos taurus]	4
gi 154425814	IGK protein [Bos taurus]	5	gi 77735883	serum amyloid P-component precursor [Bos taurus]	7	gi 296484341	TPA: protein AMBP precursor [Bos taurus]	4
gi 397740864	vitamin D binding protein [Bos taurus]	5	gi 358420619	PREDICTED: complement C4-A [Bos taurus]	6	gi 59858077	aspartate aminotransferase 1 [Bos taurus]	4
gi 114052298	apolipoprotein A-II precursor [Bos taurus]	5	gi 296475228	TPA: serpin peptidase inhibitor, clade A (alpha-1 antiproteinase, antitrypsin), member 3 [Bos taurus]	5	gi 94966811	alpha-1-acid glycoprotein precursor [Bos taurus]	4
gi 358421409	PREDICTED: keratin, type II cytoskeletal 1 [Bos taurus]	4	gi 27806741	beta-2-glycoprotein 1 precursor [Bos taurus]	5	gi 296487872	TPA: keratin 6A [Bos taurus]	4
gi 194685481	PREDICTED: keratin, type I cytoskeletal 10-like isoform 2 [Bos taurus]	4	gi 59858077	aspartate aminotransferase 1 [Bos taurus]	4	gi 29648975	TPA: CD5 molecule-like [Bos taurus]	4
gi 30466252	carbonic anhydrase 2 [Bos taurus]	4	gi 27807341	cathelicidin-1 precursor [Bos taurus]	2	gi 395268	conglutinin [Bos taurus]	3
gi 78369426	prostaglandin reductase 1 [Bos taurus]	4	gi 296480310	TPA: apolipoprotein A-I-like [Bos taurus]	2	gi 397740864	vitamin D binding protein [Bos taurus]	3
gi 41386683	beta-2-microglobulin precursor [Bos taurus]	4	gi 375065868	ceruloplasmin precursor [Bos taurus]	2	gi 114051856	keratin, type II cytoskeletal 7 [Bos taurus]	3
gi 83405800	Legumain [Bos taurus]	4	gi 78369352	complement component C9 precursor [Bos taurus]	2	gi 78369352	complement component C9 precursor [Bos taurus]	3
gi 302179501	epidermal growth factor receptor [Bos taurus]	4	gi 300797776	DNA-directed RNA polymerase I subunit RPA1 [Bos taurus]	1	gi 27807009	insulin-like growth factor-binding protein 4 precursor [Bos taurus]	2

gi 129277510	extracellular superoxide dismutase [Cu-Zn] precursor [Bos taurus]	3	gi 91982959	immunoglobulin gamma 1 heavy chain constant region [Bos taurus]	25	gi 126607	RecName: Full=Lysozyme C; AltName: Full=1,4-beta-N-acetylmuramidase C; Flags: Precursor	2
gi 114052314	plasma kallikrein precursor [Bos taurus]	3	gi 148356276	keratin, type II cytoskeletal 4 [Bos taurus]	6	gi 47564119	apolipoprotein C-III precursor [Bos taurus]	1
gi 333360891	hepatocyte growth factor activator preprotein [Bos taurus]	3	gi 22773998	immunoglobulin delta heavy chain membrane bound form [Bos taurus]	4	gi 343197026	immunoglobulin lambda light chain constant region 3 allotypic variant IGLC3c [Bos taurus]	15
gi 84000195	phosphoglycerate mutase 2 [Bos taurus]	3	gi 75832116	inter-alpha-trypsin inhibitor heavy chain H4 precursor [Bos taurus]	2	gi 310893435	immunoglobulin light chain [Bos taurus]	8
gi 94966763	haptoglobin precursor [Bos taurus]	3	gi 397740864	vitamin D binding protein [Bos taurus]	2	gi 2323384	immunoglobulin light chain variable region [Bos taurus]	7
gi 75812940	phosphatidylethanolamine-binding protein 1 [Bos taurus]	2	gi 291490675	CD44 antigen precursor [Bos taurus]	2	gi 358421409	PREDICTED: keratin, type II cytoskeletal 1 [Bos taurus]	3
gi 61888856	triosephosphate isomerase [Bos taurus]	2	gi 300795742	synaptic vesicle membrane protein VAT-1 homolog [Bos taurus]	2	gi 77735935	complement C2 precursor [Bos taurus]	3
gi 375065868	ceruloplasmin precursor [Bos taurus]	2	gi 432134242	DNA excision repair protein ERCC-6-like 2 [Bos taurus]	1	gi 45429979	spleen trypsin inhibitor 1 precursor [Bos taurus]	3
gi 358421417	PREDICTED: keratin, type II cytoskeletal 3 [Bos taurus]	2	gi 329664128	protocadherin-17 precursor [Bos taurus]	1	gi 41386685	thrombospondin-1 precursor [Bos taurus]	2
gi 156120583	arylsulfatase G [Bos taurus]	2	gi 164448719	sterile alpha motif domain-containing protein 3 [Bos taurus]	1	gi 296487901	TPA: insulin-like growth factor-binding protein 6 precursor [Bos taurus]	2
gi 27806591	glutathione peroxidase 1 [Bos taurus]	2	gi 156120521	kinesin-like protein KIFC1 [Bos taurus]	1	gi 27806907	clusterin preproprotein [Bos taurus]	2
gi 34538498	immunoglobulin heavy chain constant region [Bos taurus]	2	gi 27806751	alpha-2-HS-glycoprotein precursor [Bos taurus]	1	gi 194670528	PREDICTED: ribonuclease 4 [Bos taurus]	2
gi 15088675	immunoglobulin lambda light chain [Bos taurus]	29	gi 114051379	leucine-rich alpha-2-glycoprotein precursor [Bos taurus]	1	gi 27806751	alpha-2-HS-glycoprotein precursor [Bos taurus]	2
gi 148744128	Unknown (protein for MGC:159455) [Bos taurus]	29	gi 359070805	PREDICTED: collagen alpha-1(V) chain-like [Bos taurus]	1	gi 157954059	Fe fragment of IgG, low affinity IIc, receptor for (CD32) [Bos taurus]	2
gi 343197018	immunoglobulin lambda light chain constant region 3 allotypic variant IGLC3b [Bos taurus]	9	gi 1351907	RecName: Full=Serum albumin; AltName: Full=BSA; AltName: Allergen=Bos d 6; Flags: Precursor	821	gi 6006423	hemoglobin alpha chain [Bos taurus]	2
gi 310893435	immunoglobulin light chain [Bos taurus]	7	gi 74267962	ALB protein [Bos taurus]	702	gi 297488636	PREDICTED: protein phosphatase 1M [Bos taurus]	1
gi 296487283	TPA: hyaluronan synthase 2-like [Bos taurus]	3	gi 83764016	prepro complement component C3 [Bos taurus]	55	gi 27807335	cathelicidin-7 precursor [Bos taurus]	1
gi 187171271	dual specificity mitogen-activated protein kinase kinase 2 [Bos taurus]	2	gi 4093220	complement component 3 [Bos taurus]	55	gi 114050753	protein HP-25 homolog 1 precursor [Bos taurus]	1
gi 83764016	prepro complement component C3 [Bos taurus]	1	gi 122697593	alpha-1-acid glycoprotein precursor [Bos taurus]	42	gi 85681876	RecName: Full=Protein-lysine 6-oxidase; AltName: Full=Lysyl oxidase; Flags: Precursor	1
gi 148745450	Fibrinogen alpha chain [Bos taurus]	1	gi 114326282	serotransferrin precursor [Bos taurus]	40	gi 296487283	TPA: hyaluronan synthase 2-like [Bos taurus]	1
gi 300797661	transcription elongation factor SPT6 [Bos taurus]	1	gi 2501351	RecName: Full=Serotransferrin; Short=Transferrin; AltName: Full=Beta-1 metal-binding globulin; AltName: Full=Siderophilin; Flags: Precursor	40	gi 114051379	leucine-rich alpha-2-glycoprotein precursor [Bos taurus]	1
gi 164452943	gelsolin isoform a precursor [Bos taurus]	1	gi 84000165	complement factor 1 precursor [Bos taurus]	37	gi 1351907	RecName: Full=Serum albumin; AltName: Full=BSA; AltName: Allergen=Bos d 6; Flags: Precursor	685
gi 300795058	gamma-glutamyltransferase 5 precursor [Bos taurus]	1	gi 151556360	Unknown (protein for MGC:159378) [Bos taurus]	37	gi 154425704	ALB protein [Bos taurus]	573
gi 151554455	MSH3 protein [Bos taurus]	1	gi 343197030	immunoglobulin lambda light chain constant region 3 allotypic variant IGLC3d [Bos taurus]	26	gi 83764016	prepro complement component C3 [Bos taurus]	130
gi 157954059	Fe fragment of IgG, low affinity IIc, receptor for (CD32) [Bos taurus]	1	gi 331284120	proteoglycan 4 precursor [Bos taurus]	20	gi 2506196	RecName: Full=Beta-2-glycoprotein 1; AltName: Full=Apolipoprotein H; Short=Apo-H; AltName: Full=Beta-2-glycoprotein I; Short=B2GPI; Short=Beta(2)GPI; Flags: Precursor	88
gi 77735466	complement factor D precursor [Bos taurus]	1	gi 343197008	immunoglobulin lambda light chain constant region 2 allotypic variant IGLC2c [Bos taurus]	20	gi 6	beta-2-glycoprotein I [Bos taurus]	88
gi 1351907	RecName: Full=Serum albumin; AltName: Full=BSA; AltName: Allergen=Bos d 6; Flags: Precursor	1125	gi 134085706	keratin, type II cytoskeletal 6A [Bos taurus]	19	gi 92096965	Immunoglobulin light chain, lambda gene cluster [Bos taurus]	48
gi 74267962	ALB protein [Bos taurus]	978	gi 343197026	immunoglobulin lambda light chain constant region 3 allotypic variant IGLC3c [Bos taurus]	16	gi 139948632	immunoglobulin lambda-like polypeptide 1 precursor [Bos taurus]	45
gi 114326282	serotransferrin precursor [Bos taurus]	643	gi 163190	insulin-like growth factor binding protein-3 [Bos taurus]	14	gi 2501351	RecName: Full=Serotransferrin; Short=Transferrin; AltName: Full=Beta-1 metal-binding globulin; AltName: Full=Siderophilin; Flags: Precursor	37
gi 2506196	RecName: Full=Beta-2-glycoprotein 1; AltName: Full=Apolipoprotein H; Short=Apo-H; AltName: Full=Beta-2-glycoprotein I; Short=B2GPI; Short=Beta(2)GPI; Flags: Precursor	37	gi 27806743	protein AMBP precursor [Bos taurus]	14	gi 114326282	serotransferrin precursor [Bos taurus]	37
gi 109939993	Apolipoprotein H (beta-2-glycoprotein 1) [Bos taurus]	37	gi 2323404	immunoglobulin light chain variable region [Bos taurus]	12	gi 148745450	Fibrinogen alpha chain [Bos taurus]	16
gi 74353860	IGL@ protein [Bos taurus]	33	gi 1276627	immunoglobulin lambda light chain variable region, partial [Bos taurus]	12	gi 164414425	collagen alpha-1(II) chain isoform 1 precursor [Bos taurus]	14
gi 139948632	immunoglobulin lambda-like polypeptide 1 precursor [Bos taurus]	32	gi 148745450	Fibrinogen alpha chain [Bos taurus]	11	gi 3789962	fibrinogen A-alpha chain [Bos taurus]	14
gi 296474257	TPA: complement component 2 precursor [Bos taurus]	30	gi 3789962	fibrinogen A-alpha chain [Bos taurus]	11	gi 329665078	polyubiquitin-C [Bos taurus]	14
gi 11120280	complement component 2 precursor [Bos taurus]	30	gi 262118301	keratin, type I cytoskeletal 14 [Bos taurus]	10	gi 350537449	putative ubiquitin C variant 5 [Taeniopygia guttata]	13
gi 6006425	hemoglobin alpha chain [Bos taurus]	30	gi 116004057	keratin, type II cytoskeletal 75 [Bos taurus]	10	gi 296478548	TPA: ubiquitin C [Bos taurus]	13

gi 12206517	RecName: Full=Aspartate aminotransferase, cytoplasmic; AltName: Full=Glutamate oxaloacetate transaminase 1; AltName: Full=Transaminase A	26	gi 297474460	PREDICTED: keratin, type II cytoskeletal 1 [Bos taurus]	9	gi 28189917	similar to polyubiquitin [Bos taurus]	13
gi 154707900	fumarylacetoacetase [Bos taurus]	17	gi 296476308	TPA: keratin, type I cytoskeletal 10 [Bos taurus]	9	gi 28189839	similar to polyubiquitin [Bos taurus]	13
gi 154425761	FAH protein [Bos taurus]	17	gi 27805977	keratin, type I cytoskeletal 10 [Bos taurus]	9	gi 27806505	polyubiquitin-B [Bos taurus]	13
gi 7547266	IgG1 heavy chain constant region [Bos taurus]	16	gi 194685481	PREDICTED: keratin, type I cytoskeletal 10-like isoform 2 [Bos taurus]	9	gi 163575	polyubiquitin, partial [Bos taurus]	13
gi 119892690	PREDICTED: WASH complex subunit 7 [Bos taurus]	13	gi 358416465	PREDICTED: immunoglobulin lambda-like polypeptide 5-like [Bos taurus]	9	gi 163573	polyubiquitin, partial [Bos taurus]	13
gi 343197004	immunoglobulin lambda light chain constant region 2 allotypic variant IGLC2b [Bos taurus]	13	gi 343196996	immunoglobulin lambda light chain constant region 2 allotypic variant IGLC2a [Bos taurus]	9	gi 110282963	RecName: Full=Folate receptor alpha; Short=FR-alpha; AltName: Full=Folate receptor 1; AltName: Full=Folate-binding protein 1; Short=FBP; AltName: Full=Milk folate-binding protein; Flags: Precursor	11
gi 343197008	immunoglobulin lambda light chain constant region 2 allotypic variant IGLC2c [Bos taurus]	11	gi 157427776	keratin, type I cytoskeletal 17 [Bos taurus]	9	gi 2323374	immunoglobulin light chain variable region [Bos taurus]	11
gi 2323380	immunoglobulin light chain variable region [Bos taurus]	10	gi 296489775	TPA: CDS molecule-like [Bos taurus]	8	gi 2323376	immunoglobulin light chain variable region [Bos taurus]	11
gi 2323376	immunoglobulin light chain variable region [Bos taurus]	10	gi 2323380	immunoglobulin light chain variable region [Bos taurus]	8	gi 2323386	immunoglobulin light chain variable region [Bos taurus]	11
gi 2323374	immunoglobulin light chain variable region [Bos taurus]	10	gi 2323376	immunoglobulin light chain variable region [Bos taurus]	8	gi 296478557	TPA: ubiquitin B-like [Bos taurus]	10
gi 75812938	dipeptidyl peptidase 1 precursor [Bos taurus]	9	gi 358421417	PREDICTED: keratin, type II cytoskeletal 3 [Bos taurus]	8	gi 163190	insulin-like growth factor binding protein-3 [Bos taurus]	10
gi 359064628	PREDICTED: protein piccolo-like [Bos taurus]	9				gi 296479849	TPA: folate receptor 1-like [Bos taurus]	10
						gi 2323400	immunoglobulin light chain variable region [Bos taurus]	10
						gi 296486756	TPA: complement factor I [Bos taurus]	8
						gi 975844	immunoglobulin lambda light chain variable region, partial [Bos taurus]	8